Wave-Guiding Analysis of Annular Core Geometry Metal-Clad Semiconductor Nano-Lasers

Zubaida Abdul Sattar, *Student Member, IEEE*, Zengbo Wang, and K. Alan Shore, *Senior Member, IEEE*

***Abstract*— Numerical modeling of cylindrical semiconductor nano-lasers has been undertaken accommodating local gain variations in the active region of the device. Analysis is performed using both the cylindrical transfer matrix method and the finite element method. Calculations have thereby been performed of the modal gain and the lasing condition for the device. The model has been applied to annular active core structures and a comparison has been made of the requirements for achieving lasing via the excitation of TE_{01} and TM_{01} modes. For representative structures, it is shown that TE and TM mode lasing can be supported in devices having cavity lengths in the order of 1 and 60 μm, respectively.**

***Index Terms*— Inner core, lasing, material gain, metal-clad, modal gain, nano-laser, outer core.**

I. Introduction

ADVANCES in semiconductor laser technology have been pursued with a view to the implementation of integrated photonic components. In this context a specific challenge is to design and fabricate ultra-compact semiconductor lasers amenable to high-density photonic integration. Crucial issues in this regard are the identification of structures which enable effective light confinement and thereby enable lasing in nano-scale cavities.

The design process for advanced laser structures is reliant on accurate modeling of the physical processes underpinning the operational characteristics of candidate semiconductor nano-laser designs. Moreover the drive towards miniaturization relies on the utilization of novel structural features. In general the modeling of such aspects requires the adoption of numerical techniques in order to provide accurate predictions of the behaviour of proposed nano-lasers.

A variety of nano-scale lasers have been explored in recent years, including: micropost [1] nanopillar and bowtie [2]–[4], Fabry-Perot [5], nanowire [6], spaser-based [7], and nano patch [8] lasers. Cylindrical semiconductor metal-clad nano-lasers offer an improvement to the confinement loss and modal gain for such applications. Some improvements can be made through the optimization of the geometry and materials and by reducing structural imperfections. However the lower limit for optical losses is imposed by the physical properties of the metal and can only be balanced by introducing optical gain into the structure.

Numerical analysis of metal-clad nano-lasers has been developed e.g., by Maslov *et al*. who studied the GaAs nanowires surrounded by an infinitely thick silver (Ag) cladding as a means to effect size reduction of cylindrical nanowire lasers [9]; Vivek *et al*. investigated the effect of metal cladding on the coupling of modes emphasizing their mode confinement and loss characteristics [10]. Recent numerical studies give insight into the gain properties for a uniform core structure [11], [12]. In a previous publication, we have determined the lasing condition for a two layer active core model. The core was divided into inner and outer core with variation in the material gain is only considered in the outer core region [13].

For the work presented here we consider a more realistic model with material gain variation in the core, of prescribed optical properties and of specifically defined optical gain. In that context, a numerical model that emulates a cylindrical metal-clad nano-laser using cTMM (cylindrical transfer matrix method) has been used for this work. The technique used follows that of Yeh and Yariv [14], [15] which studied passive distributed Bragg fibers. The advantage of this approach is that it is a simple and straightforward way to analyse waveguide structures. Specifically it requires less computational time compared to techniques such as Finite Element Method (FEM) and Finite Difference Time Domain (FDTD). In contrast, the aim of the present work is to explore the lasing conditions for TE and TM mode of metal-clad nano-lasers by incorporating annular core geometry.

The HE_{11}, TM_{01} and TE_{01} are the lowest order modes supported by the nanolaser structure considered here. The TE_{01} mode is mostly confined in the core because of the metal cladding. High confinement factor which can exceed unity has been reported [16] resulting in high modal gain. Also the group velocity reduces, allowing the modal gain to exceed the material gain [17]. The TM_{01} and HE_{11} modes are known as the Surface Plasmon Polariton (SPP) modes [18]–[20] which are less confined to the core. We may identify two kinds of TM_{01} SPP modes: core–metal surface guided modes and air–metal surface guided modes [21], [22]. The modes guided at the air-metal interface are known as long range surface plasmon modes (considered in this work) which are of much practical interest. On the other hand the core-metal surface guided modes experience high losses and may have reduced applications potential and is therefore not considered here.

Manuscript received July 26, 2013; revised October 18, 2013; accepted November 13, 2013. Date of publication November 20, 2013; date of current version December 4, 2013. The work of Z. A. Sattar was supported in part by the School of Electronic Engineering, Bangor University, Wales, U.K., and in part by the Memon Communities in Pakistan.

The authors are with the School of Electronic Engineering, Bangor University, Wales LL57 1UT, U.K. (e-mail: z.a.sattar@bangor.ac.uk; z.wang@bangor.ac.uk; k.a.shore@bangor.ac.uk).

Color versions of one or more of the figures in this paper are available online at http://ieeexplore.ieee.org.

Digital Object Identifier 10.1109/JQE.2013.2291662

The TM_{01} air-metal mode has a higher gain than the HE_{11} mode [11]. Hence here work is undertaken on TE_{01} and TM_{01} air-metal modes.

Such nano-lasers are anticipated to exhibit enhanced dynamical performance which may arise from a combination of physical factors including enhanced modal refractive indices and Purcell cavity-enhanced spontaneous emission. However in complementary work [23] on the dynamical performance of metal-clad nano-lasers it was shown by means of a simple analysis that the direct-current modulation bandwidth of such lasers may suffer deleterious effects due to those factors.

In order to bench mark the laser performance we have examined the operating conditions for the low order TE_{01} and air-metal TM_{01} SPP mode which have the potential to lase [11]. The TM_{01} is a lossy mode as it is guided mostly in the air-metal interface rather in the core active region, where the TE_{01} mode resides mostly in the core. The potential advantage of TM_{01} mode in metal-clad nanolasers is reduced cross-coupling between closely spaced devices on a photonic integrated circuit [10].

The approach adopted is to take into account the spatial profile of the optical gain as a means both for optimizing lasing operation and as a step towards a fully self-consistent theoretical 2D model of such structures. The paper is organized as follows. Firstly, the laser structure is discussed and the mode calculation technique is given. Results using the methodology are then presented. Finally, conclusions are drawn from those results.

II. Laser Structure and 2D Model

The structure under consideration is a cylindrical annular core metal-clad nano-laser. In previous work such a structure has been studied assuming a uniform core [10]–[12]. In order to take into account spatial variations in gain in the active region of such a structure an annular core geometry is utilized. The cross-section of such a structure is illustrated in Fig. 1.

The key elements of the structure are the core semiconductor region and the metal cladding. The analysis methodology adopted here is of general application but for the work presented here it is assumed that the metal-clad structure is surrounded by air. It is straightforward to examine alternative configurations and notably the use of alternative surrounding media. Following earlier work the core semiconductor material is assumed to be $In_{0.53}Ga_{0.47}As$ with a refractive index of 3.53 at the operating wavelength $\lambda_o = 1.55\mu$m [24]. The metal cladding is taken to be gold with a refractive index of 0.52 – j10.74 [25] and the thickness of metal-clad is assumed to be 20 nm [18].

The model which has been developed for this work allows for the definition of an arbitrary number of layers in the active layer core semiconductor region as well as in the cladding region. This utility has been developed in order to explore combinations of gain profiles and/or surrounding media. However, for the specific calculations performed here, the core semiconductor is considered to be comprised of N annular regions of radius r with differing material gains, with

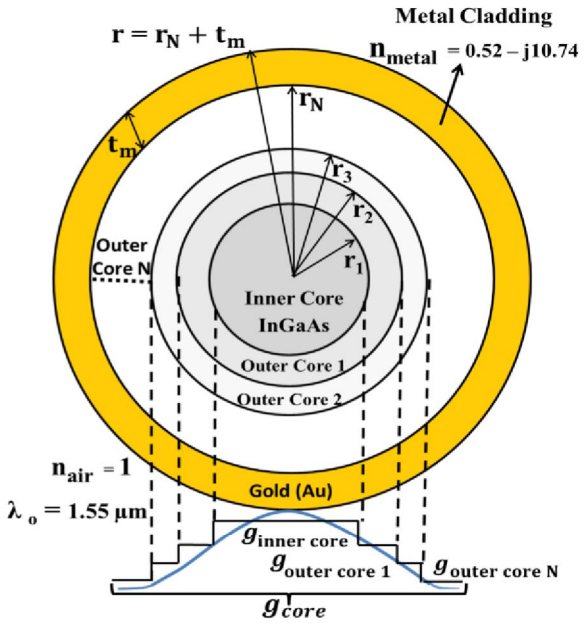

Fig. 1. Cross-section and Schematic of the cylindrical semiconductor annular core metal-clad nano-laser.

the index profile n in (1),

$$n(r) = \begin{cases} n_{inner\ core} & 0 \le r < r_1 \\ n_{outer\ core\ 1} & r_1 \le r < r_2 \\ \quad . & \\ \quad . & \\ n_{outer\ core\ N} & r_{N-1} \le r < r_N \\ n_{metal} & r_N \le r < r_N + t_m \\ n_{air} & r \ge r_N + t_m \end{cases} \tag{1}$$

Where, N is the number of outer core annuli in the active core region. The refractive index profile of active core annuli includes a material gain profile such that,

$$g_{inner\ core} > g_{outer\ core\ 1} > g_{outer\ core\ 2} \cdots > g_{outer\ core\ N}$$

The method of pumping in lasers determines the gain in the core active region. Experimental study of nano-lasers has been performed using the optical pumping and electrical pumping [5]–[8]. It is challenging to achieve highly doped p-n junctions in nanowires that can offer electrical excitation [10]. The work carried out here does not rely on any particular pumping method. As discussed in section III, the simulations undertaken here are applicable to any pumping which results, due to carrier diffusion, in the material gain having a Gaussian profile. Therefore, for an $In_{0.53}Ga_{0.47}As$ core with gain included (g_{core}) the index profile for N annuli becomes,

$$\begin{aligned} n_{inner\ core} &= 3.53 + j\frac{g_{inner\ core}}{2\gamma_o} \\ n_{outer\ core\ 1} &= 3.53 + j\frac{g_{outercore\ 1}}{2\gamma_o} \\ &\ . \\ &\ . \\ &\ . \\ n_{outer\ core\ N} &= 3.53 + j\frac{g_{outercore\ N}}{2\gamma_o} \end{aligned}$$

Where, γ_o is the propagation constant in free space,

$$\gamma_o = \frac{2\pi}{\lambda_o} \tag{2}$$

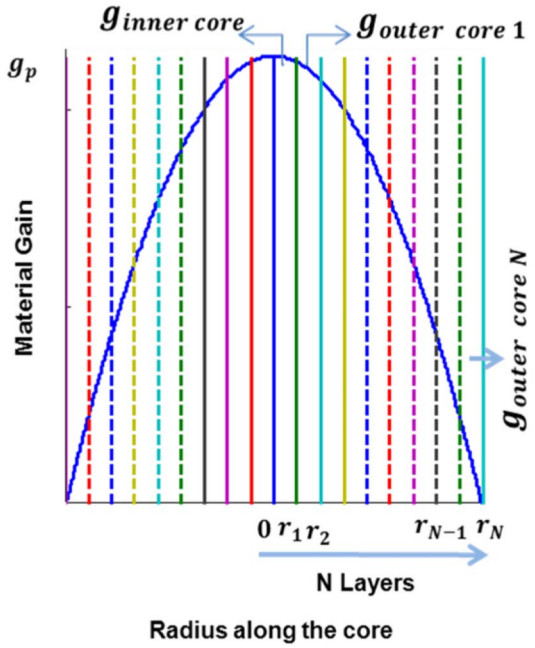

Fig. 2. Schematic of the Material Gain for N Layers in the Core.

n_{metal} and n_{air} is the refractive index of gold and air respectively and t_m is the thickness of metal cladding. λ_o is the wavelength of propagation.

III. Gain Profile

To evaluate the overall modal gain of the lower order TE mode and TM SPP mode, we represent the material gain profile in the active region using (3). As indicated in the previous sub-section the simulations described here assume that, due to the diffusion of carriers, the material gain profile has a Gaussian distribution [26].

$$g_{core} = g_p e^{(-r^2/2\sigma^2)} \tag{3}$$

Where, g_p is the peak material gain, and g_{core} varies along the radius of the core $0 \leq r \leq r_N$ and σ is the carrier diffusion length.

As shown in Fig. 2, the material gain varies along the radius of the core. For spatial profiling of the material gain, the core is divided into N layers. The gain in each layer is evaluated as an average of the values of the material gain at their respective boundaries, such that using (3) we have:

$$g_{inner\ core} = \frac{g_p}{2}\left(e^{-\left(\frac{r_0^2}{2\sigma^2}\right)} + e^{-\left(\frac{r_1^2}{2\sigma^2}\right)}\right)$$
$$g_{outer\ core\ 1} = \frac{g_p}{2}\left(e^{-\left(\frac{r_1^2}{2\sigma^2}\right)} + e^{-\left(\frac{r_2^2}{2\sigma^2}\right)}\right)$$
$$\vdots$$
$$g_{outer\ core\ N} = \frac{g_p}{2}\left(e^{-\left(\frac{r_{N-1}^2}{2\sigma^2}\right)} + e^{-\left(\frac{r_N^2}{2\sigma^2}\right)}\right)$$

The overall modal gain, G is evaluated using (4):

$$G = \frac{4\pi}{\lambda_o} Im(n_{eff}) \tag{4}$$

Where, $Im(n_{eff})$ is the imaginary part of the effective refractive index of the mode.

IV. Waveguide Analysis Technique

In this section we introduce the cTMM for the cylindrical annular core metal-clad nano-laser, which is used to compute the mode characteristics as well as the gain and device length to support lasing action. For eigen-mode analysis of the structure presented in Fig. 1, we use cTMM to represent and solve the boundary conditions [14], [15]. We consider the z axis as the direction of propagation and therefore, all field components within the cylindrical structure can be represented in the form,

$$\zeta\,(r,\theta,z,t) = \zeta\,(r,\theta)\,e^{i(\beta z-\omega t)} \tag{5}$$

Where ζ represents the field components in the structure, i.e., $E_z, E_r, E_\theta, H_z, H_r, H_\theta$. ω being the angular frequency and β is the mode propagation constant. The field propagates within the structure of radius r radially with angle θ along the direction of propagation z at time t.

$$E_r = \frac{1}{\gamma}\left(j\beta E_z^{'}(r) + \frac{j\omega\mu}{r} H_z^{'}(\theta)\right)$$
$$E_\theta = \frac{1}{\gamma}\left(\frac{j\beta}{r} E_z^{'}(\theta) - j\omega\mu H_z^{'}(r)\right)$$
$$H_r = \frac{1}{\gamma}\left(j\beta H_z^{'}(r) - \frac{j\omega\epsilon}{r} E_z^{'}(\theta)\right)$$
$$H_\theta = \frac{1}{\gamma}\left(\frac{j\beta}{r} H_z^{'}(\theta) + j\omega\epsilon E_z^{'}(r)\right) \tag{6}$$

Where, μ, ϵ are the permeability and permittivity of the medium and γ is propagation constant in the medium as in (7),

$$\gamma = \sqrt{\gamma_o^2\mu\epsilon - \beta^2} \tag{7}$$

Where, γ_0 is the propagation constant in free space as in (2). For the analysis of the structure, the transverse field component for the TM and TE mode is expressed in terms of E_z and H_z respectively,

$$E_{zi} = \left[U_i J_o(\gamma_i r_i) + V_i Y_o(\gamma_i r_i)\right] \tag{8}$$
$$H_{zi} = \left[W_i J_o(\gamma_i r_i) + Q_i Y_o(\gamma_i r_i)\right] \tag{9}$$

Where J_o and Y_o are the zero order Bessel functions of the first and second kind respectively. U_i, V_i, W_i, Q_i are field amplitudes, the indices $i = 1, 2, 3 \ldots N, N+1, N+2$ represents the appropriate region of the structure as shown in Fig. 3 and γ_i is represented in the form of material and modal gain as in (10)

$$\gamma_i = \gamma_o\sqrt{\left(Re(n_i) \pm j\frac{g_i}{2\gamma_o}\right)^2 - \left(Re(n_{eff}) \pm j\frac{G}{2\gamma_o}\right)^2} \tag{10}$$

Where,
$\mathbf{Re(n_i)}$ is the real part of refractive index of each layer,

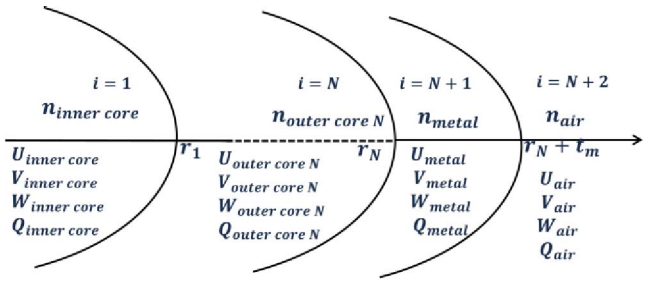

Fig. 3. Layer interface for the annulus core structure. Where i defines the semiconductor dielectric annuli, the metal layer and the outer most cladding i.e., air.

G is the modal gain/loss, which is evaluated using the cTMM, $\mathbf{g_i}$ is the material gain for the semiconductor core and loss for the metal.

$\mathbf{Re}(\mathbf{n}_{\mathit{eff}})$ is the real part of the effective refractive index of the mode.

The boundary conditions at each interface are that E_z, E_θ, H_z and H_θ are continuous. In our approach the boundary conditions are satisfied by using a matrix A_i and B_i, which links the field amplitudes with adjacent layers i.e., U_i, V_i, W_i, Q_i to $U_{i+1}, V_{i+1}, W_{i+1}, Q_{i+1}$ For TM mode

$$\begin{pmatrix} U_{i+1} \\ V_{i+1} \end{pmatrix} = A_i \begin{pmatrix} U_i \\ V_i \end{pmatrix} \tag{11}$$

For TE mode

$$\begin{pmatrix} W_{i+1} \\ Q_{i+1} \end{pmatrix} = B_i \begin{pmatrix} W_i \\ Q_i \end{pmatrix} \tag{12}$$

The matrix for the TM and TE modes that links the field parameters from the first layer i.e., inner core to the outer most cladding i.e., air, can be represented as,

$$\begin{pmatrix} U_{air} \\ V_{air} \end{pmatrix} = M \begin{pmatrix} U_{inner\ core} \\ V_{inner\ core} \end{pmatrix} \tag{13}$$

$$\begin{pmatrix} W_{air} \\ Q_{air} \end{pmatrix} = P \begin{pmatrix} W_{inner\ core} \\ Q_{inner\ core} \end{pmatrix} \tag{14}$$

Where M and P are formed by the matrix multiplication of the matrices A_i & B_i for layers $i = 1, 2, 3.....N, N+1, N+2$ such that,

$$M = A_1 A_2 A_3 \ldots\ldots\ldots A_{i-1} \tag{15}$$

$$P = B_1 B_2 B_3 \ldots\ldots\ldots B_{i-1} \tag{16}$$

Where the boundary interface $A_1 A_2 \ldots\ldots A_{i-1}$ in (15) and $B_1 B_2 \ldots\ldots B_{i-1}$ in (16) are calculated by

$$A_i = m_{TM}^{-1}(i+1, r_i)\, m_{TM}(i, r_i) \tag{17}$$

$$B_i = m_{TE}^{-1}(i+1, r_i)\, m_{TE}(i, r_i) \tag{18}$$

m_{TE} and m_{TM} in (17) and (18) are in the form,

$$m_{TE}(i, r_i) = \begin{bmatrix} J_o(\gamma_i r_i) & Y_o(\gamma_i r_i) \\ \frac{\omega}{\beta \gamma_i} J_o'(\gamma_i r_i) & \frac{\omega}{\beta \gamma_i} Y_o'(\gamma_i r_i) \end{bmatrix} \tag{19}$$

$$m_{TM}(i, r_i) = \begin{bmatrix} J_o(\gamma_i r_i) & Y_o(\gamma_i r_i) \\ \frac{\omega n_i^2}{\beta \gamma_i} J_o'(\gamma_i r_i) & \frac{\omega n_i^2}{\beta \gamma_i} Y_o'(\gamma_i r_i) \end{bmatrix} \tag{20}$$

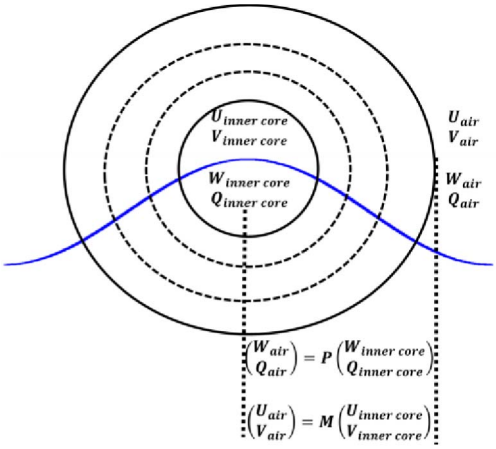

Fig. 4. Representation for the boundary condition between the inner core and the outer most cladding.

The elements of (19) and (20) are relatively involved expressions that are not re-produced here. In order to obtain a finite field at the centre of the inner core and a decaying field in the outer most dielectric, as shown in Fig. 4, we require,

$$\begin{aligned} V_{inner\ core} = 0,\, Q_{inner\ core} = 0,\, V_{air} \\ = jU_{air}\ \&\ Q_{air} = jW_{air} \end{aligned} \tag{21}$$

Hence, after applying boundary conditions using (21) in (11) and (12) we have,

For TM mode

$$\begin{pmatrix} U_{air} \\ jU_{air} \end{pmatrix} = \begin{pmatrix} M_{11} & M_{12} \\ M_{21} & M_{22} \end{pmatrix} \begin{pmatrix} U_{inner\ core} \\ 0 \end{pmatrix} \tag{22}$$

For TE mode

$$\begin{pmatrix} W_{air} \\ jW_{air} \end{pmatrix} = \begin{pmatrix} P_{11} & P_{12} \\ P_{21} & P_{22} \end{pmatrix} \begin{pmatrix} W_{inner\ core} \\ 0 \end{pmatrix} \tag{23}$$

Re-arranging (22) and (23), we have, For TM mode

$$\left.\begin{aligned} U_{inner\ core} M_{11} - U_{air} = 0 \\ U_{inner\ core} M_{21} - jU_{air} = 0 \end{aligned}\right\} \tag{24}$$

For TE mode

$$\left.\begin{aligned} W_{inner\ core} P_{11} - W_{air} = 0 \\ W_{inner\ core} P_{21} - jW_{air} = 0 \end{aligned}\right\} \tag{25}$$

Writing (24) and (25) in matrix form, we have,

$$\begin{pmatrix} M_{11} & -1 \\ M_{21} & -j \end{pmatrix} \begin{pmatrix} U_{inner\ core} \\ U_{air} \end{pmatrix} = 0 \tag{26}$$

$$\begin{pmatrix} P_{11} & -1 \\ P_{21} & -j \end{pmatrix} \begin{pmatrix} W_{inner\ core} \\ W_{air} \end{pmatrix} = 0 \tag{27}$$

We then obtain the eigen-equations by taking the determinant of the matrix in (26) and (27) equal to zero.

$$\begin{vmatrix} M_{11} & -1 \\ M_{21} & -j \end{vmatrix} = 0 \tag{28}$$

$$\begin{vmatrix} P_{11} & -1 \\ P_{21} & -j \end{vmatrix} = 0 \tag{29}$$

In this case the Eigen equation for the TM and TE mode becomes;

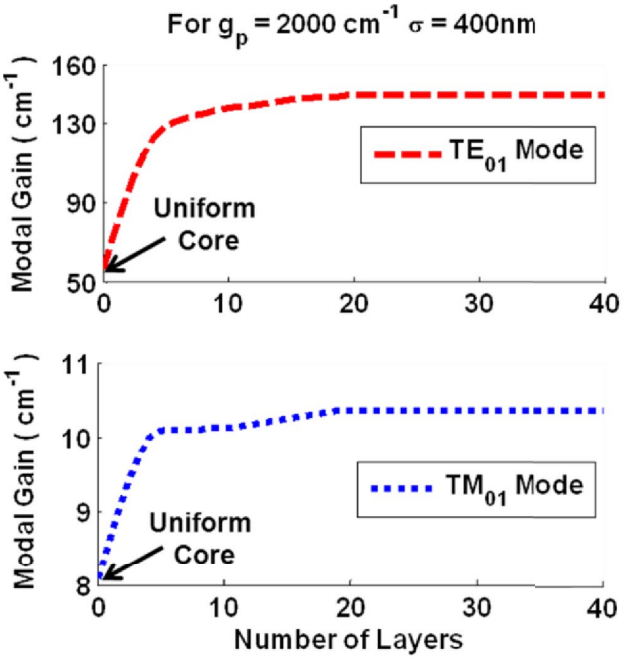

Fig. 5. Effect of increased layers in the core to the Modal Gain.

For TM;

$$M_{21} - jM_{11} = 0 \tag{30}$$

For TE;

$$P_{21} - jP_{11} = 0 \tag{31}$$

The eigenvalue equations in (30) and (31) were then used to evaluate the optical gain of the TE and TM modes using the Secant Iteration Method and hence the lasing condition for the structure is determined. Simulations were performed using MATLAB.

V. Results

The principal aim of this paper is to evaluate the optical gain and lasing condition using annular core geometry in a cylindrical metal-clad nano-laser. It has been noted that for the TM_{01} mode the maximum gain is achieved at cut off radius [9]. On the other hand for the TE modes the gain will increase with device radius [11]. As such a comparison is made between the lower order TE and TM modes at their respective cut-off radii. For the analysis carried out here the overall radius r_N of the core for the TE_{01} and TM_{01} mode is therefore assumed to be 250 nm and 180 nm respectively.

To evaluate the effect of spatial profiling of the material gain in the core to the overall modal gain of the structure, cTMM is used. For the gain profile in (3) a peak material gain $g_p = 2000\text{cm}^{-1}$, a diffusion length $\sigma = 400$ nm [27] is used. The effect of increasing the number of layers (N) on the modal gain is examined for the gain profile as shown in Fig. 2. The overall modal gain is evaluated using (4).

Fig. 5 shows the effect of the increasing number of layers on the evaluation of modal gain using cTMM. For a uniform core, the material gain in the core will be the average of the peak value g_p to the minimum value of the material gain at r_N for the gain profile defined in (3). The evaluated modal gain for a uniform core is 50cm^{-1} for the TE_{01} mode and 8cm^{-1} for the TM_{01} mode as shown in Fig. 5. The lower value of the modal gain for TM_{01} mode reflecting its lossy nature.

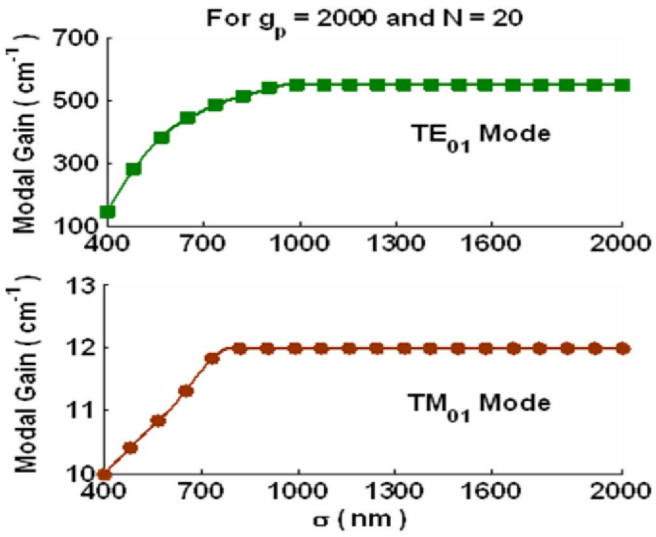

Fig. 6. Modal Gain dependence upon increased diffusion length (σ).

When additional layers are introduced to obtain a better approximation of the gain profile the overall modal gain increases because values of the local gain intermediate between the maximum and minimum are taken into account. For $N \geq 20$ the gain remains constant as shown in Fig. 5.

For further analysis the results obtained here are therefore carried out using $N = 20$. Attention is now turned to the effect of variation of diffusion length σ on the modal gain. The diffusion length of the considered semiconductor material is therefore varied from 400 nm–2000 nm [27]–[29] and the modal gain is evaluated for a peak material gain $g_p = 2000\text{cm}^{-1}$. For the gain distribution considered here, an increase in the diffusion length reduces the gain variation in the core.

For diffusion lengths of order 1μm, an essentially uniform gain is obtained across the active core. The greater variation in the gain profile for smaller diffusion lengths naturally results in a reduced modal gain, as shown in Fig. 6, for both the TE_{01} and the TM_{01} mode. For the considered structure, values of diffusion length (σ) less than 1μm, material gain (carrier density) variation is taken into account. The modal gain variation becomes insignificant for σ greater than 1μm. Fig. 6 also shows that there is an increase in the modal gain for the TE_{01} mode compared to that of the TM_{01} mode, as TM_{01} is less confined to the core as discussed above.

Table I summarizes the modal gain and lasing lengths for the device parameters in the cases of diffusion lengths of 400 nm, 600 nm and 1000 nm and for a peak material gain of 2000cm^{-1}.

Using both cTMM and the Finite Element Method (FEM) calculations have been performed of the modal gain of the TE_{01} and TM_{01} modes. Here use has been made of peak material gains in the range 2000cm^{-1} to 6000cm^{-1} [24], [30] and a diffusion length of 400 nm.

TABLE I

DEVICE SPECIFICATIONS FOR THE TE_{01} MODE FOR $r_N = 250$ nm AND TM_{01} MODE FOR $r_N = 180$ nm AT $N = 20$

g_p(cm^{-1}) / σ	Overall Modal Gain (cm^{-1})						Device Length (μm)					
	400nm		600nm		1000nm		400nm		600nm		1000nm	
	TE mode	TM mode	TE mode	TM mode	TE mode	TM mode	TE mode	TM mode	TE mode	TM mode	TE mode	TM mode
2000	144	10	408	11	550	12	81	1126	29	1015	21	965
3000	3108	53	3504	54	3716	55	4	222	3	215	3	212
4000	6068	94	6595	97	6877	98	2	123	2	121	2	119
5000	9017	136	9671	139	10021	140	1	86	1	84	1	83
6000	11946	177	12724	180	13139	182	1	66	1	65	1	64

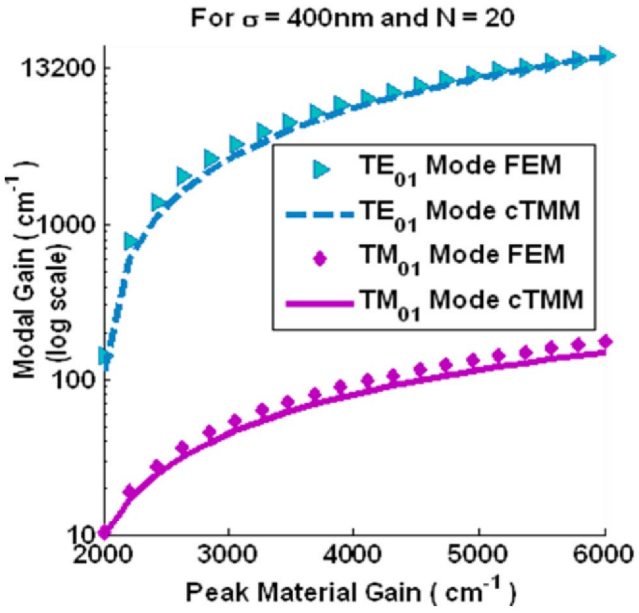

Fig. 7. Modal Gain vs Peak Material Gain for TE_{01} and TM_{01} mode evaluated using the Finite Element Method (FEM) and Cylindrical Transfer Matrix Method (cTMM).

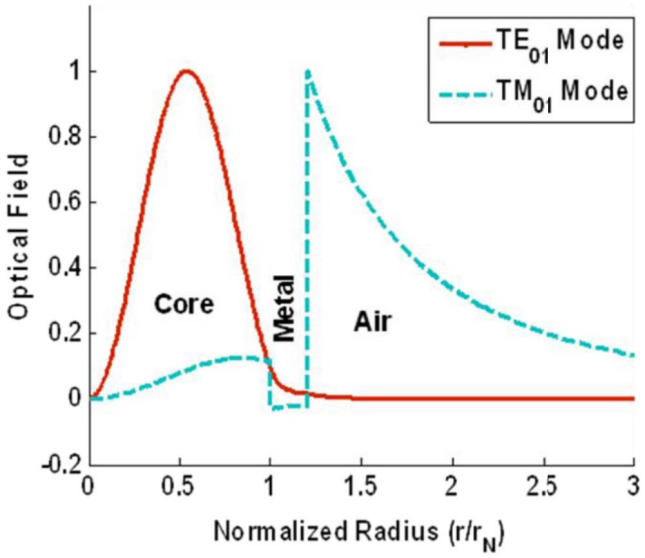

Fig. 8. Optical field for the TE_{01} and TM_{01} modes.

Fig. 7 shows that for an overall device radius of 250 nm the TE_{01} has a lower modal gain at peak material gain of 2000cm^{-1} and for the values of the peak material gain $g_p \geq 3000\text{cm}^{-1}$ we observe higher modal gain than that of the peak material gain. It is seen from Fig. 7 that similar predictions are obtained using both the cTMM approach alter the Finite Element Method.

The mode confinement factor has been evaluated using [10]. It is observed that increasing the number of layers in the core has little effect on the calculated confinement factor which is in the range 3.1 to 3.15 for the TE_{01} mode and 0.041 to 0.042 for TM_{01} mode. It is pointed out that the TM_{01} mode resides mostly in air rather in the core [21], [22] as shown by the optical field of TM_{01} and TE_{01} mode in Fig. 8.

Guided by the results shown in Fig. 7, attention is now given to the determination of the cavity lengths required to sustain lasing. The lasing condition depends on the modal gain, loss and the reflectivity of the laser facet. In the absence of accurate estimates of the loss, use is made of a simplified form of the lasing condition to determine the device length L, as:

$$L = \frac{1}{G} \ln\left(\frac{1}{R}\right) \tag{32}$$

there by obtaining a best-case estimate of the device length.

Here, G is the modal gain and R is the reflectivity of the laser. For a conventional laser diode, the reflectivity from its facets is given by the Fresnel equation. This equation is not strictly applicable for nano lasers as the diameter of the core is smaller than the lasing wavelength and due to diffraction at the edges calculation of the modal reflectivity is quite challenging [31].

Exact calculation of the facet reflectivities of such structures requires careful account to be taken of the precise structure and notably the presence or otherwise of surrounding metallic layers. In the present case, it is simply assumed that the facet reflectivity is determined by the change in dielectric constant between the semiconductor material and the surrounding medium assumed to be air. For the case examined here the facet reflectivity is R $\simeq$ 0.31.

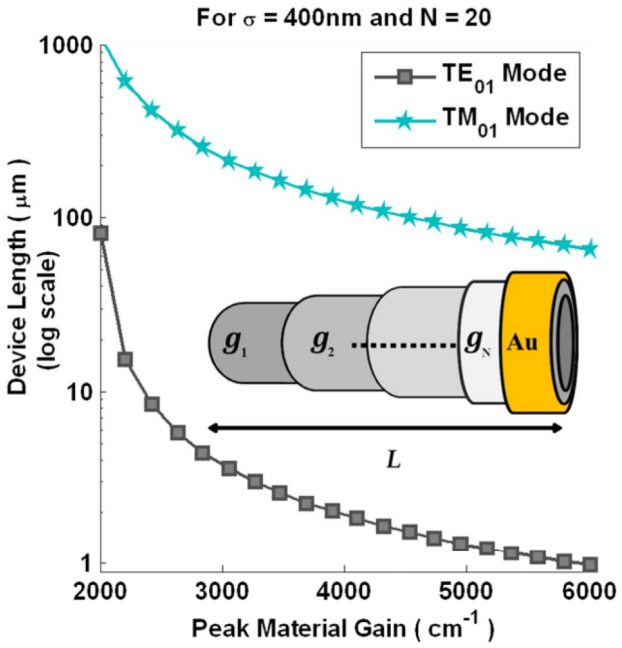

Fig. 9. Device Length vs Peak Material Gain for TE_{01} and TM_{01} mode.

Fig. 9 shows the device length for structures operating at TE_{01} mode and TM_{01} mode. It is remarked that due to the smaller gain achieved by the TM_{01} mode, the relevant cavity lengths are very sensitive to losses. In contrast the predicted cavity lengths for the TE_{01} mode are not greatly changed even when significantly higher waveguide losses are taken into account.

It is observed that as the peak material gain increases the length of the device decreases. Furthermore as the mode becomes more confined inside the core the modal gain is enhanced thus reducing the device length required to achieve lasing. Recent experimental results show that in InGaAs-based nanolasers TE mode lasing can be achieved for a device length of 0.9μm [32]. Fig. 9 shows that devices supporting TE_{01} and TM_{01} modes having cavity lengths of order 1μm and 60μm respectively appear to have the potential to support lasing action as summarized in Table I.

VI. Conclusion

In summary, we have reported an investigation using both analytical and numerical techniques of the lasing characteristics of cylindrical metal-clad nano-laser. The model which has been utilized for this purpose allows for variations of the material gain in the active core to be taken into account. Analysis is performed for TE and TM modes at their respective cut off radii. It is found that for the TE_{01} mode devices of lengths of order 1 μm have the potential to lase whereas for the TM_{01} mode device lengths of order 60 μm are needed to achieve lasing. The model developed here provides the basis for more detailed nano-laser design and specifically is capable of extension to provide a self-consistent analysis of the wave-guiding and lasing properties of such metal-clad cylindrical nano-lasers.

References

[1] M. Pelton, J. Vuckoviá, G. Solomon, C. Santori, B. Zhang, J. Plant, *et al.*, "An effcient source photons: Single quantum dot in a micropost microcavity," *Phys. E*, vol. 17, pp. 564–567, Apr. 2003.
[2] N. Yu, E. Cubukcu, L. Diehl, D. Bour, S. Corzine, J. Zhu, *et al.*, "Bowtie plasmonic quantum cascade laser antenna," *Opt. Exp.*, vol. 15, no. 20, pp. 13272–13281, Oct. 2007.
[3] S. W. Chang, C. Y. A. Ni, and S. L. Chuang, "Theory for bowtie plasmonic nanolasers," *Opt. Exp.*, vol. 16, no. 14, pp. 10580–10595, Jul. 2008.
[4] M. T. Hill, Y. S. Oei, B. Smalbrugge, Y. Zhu, T. de Vries, P. J. van Veldhoven, *et al.*, "Lasing in metallic-coated nanocavities," *Nature Photon.*, vol. 1, pp. 589–594, Oct. 2007.
[5] M. T. Hill, M. Marell, E. S. P. Leong, B. Smalbrugge, Y. Zhu, M. Sun, *et al.*, "Lasing in metal-insulator-metal sub-wavelength plasmonics waveguides," *Opt. Exp.*, vol. 17, no. 13, pp. 11107–11112, Jun. 2009.
[6] R. F. Oulton, V. J. Sorger, T. Zentgraf, R. M. Ma, C. Gladden, L. Dai, *et al.*, "Plasmon lasers at deep subwavelength scale," *Nature*, vol. 461, pp. 629–632, Oct. 2009.
[7] M. A. Noginov, G. Zhu, A. M. Belgrave, R. Bakker, V. M. Shalaev, E. E. Narimanov, *et al.*, "Demonstration of a spaser-based nanolaser," *Nature*, vol. 460, pp. 1110–1113, Aug. 2009.
[8] K. Yu, A. Lakhani, and M. C. Wu, "Subwavelength metal-optic semiconductor nanopatch lasers," *Opt. Exp.*, vol. 18, no. 9, pp. 8790–8799, Apr. 2010.
[9] A. V. Maslov and C. Z. Ning, "Size reduction of a semiconductor nanowire laser by using metal coating," *Proc. SPIE*, vol. 6468, pp. 646801-1–646801-7, Mar. 2007.
[10] V. Krishnamurthy and B. Klein, "Theoretical investigation of metal cladding for nanowire and cylindrical micropost lasers," *IEEE J. Quantum Electron.*, vol. 44, no. 1, pp. 67–74, Jan. 2008.
[11] K. Ikeda, Y. Fainman, K. A. Shore, and H. Kawaguchi, "Modified long range surface plasmon polariton modes for laser nano resonators," *J. Appl. Phys.*, vol. 110, no. 6, pp. 063106-1–063106-6, Sep. 2011.
[12] Z. A. Sattar and K. A. Shore, "Design analysis of ultra-short cavity silver-clad semiconductor nano-lasers," in *Proc. 10th Int. Conf. CLEO-PR OECC/PS*, Kyoto, Japan, Jul. 2013, pp. 1–2.
[13] Z. A. Sattar and K. A. Shore, "Spatial profiling of optical gain for optimizing lasing in plasmonic nano-lasers," *J. Eur. Opt. Soc. Rapid Publication*, vol. 8, pp. 13045-1–13045-6, Jul. 2013.
[14] P. Yeh, A. Yariv, and E. Marom, "Theory of Bragg fiber," *J. Opt. Soc. Amer.*, vol. 68, no. 9, pp. 1196–1201, Sep. 1978.
[15] P. Yeh, *Optical Waves in Layered Media*. New York, NY, USA: Wiley, 1988.
[16] A. V. Maslov and C. Z. Ning, "Modal gain in a Semiconductor nanowire laser with anisotropic bandstructure," *IEEE J. Quantum Electron.*, vol. 40, no. 10, pp. 1389–1397, Oct. 2004.
[17] D. B. Li and C. Z. Ning, "Giant modal gain, amplified surface plasmon-polariton propagation, and slowing down of energy velocity in a metal-semiconductor-metal structure," *Phy. Rev. B.*, vol. 80, no. 15, pp. 153304-1–153304-4, Oct. 2009.
[18] G. Winter, S. Wedge, and W. L. Barnes, "Can lasing at visible wavelengths be achieved using low-loss long-range surface plasmon-polariton mode?" *New J. Phys.*, vol. 8, no. 125, pp. 1–14, 2006.
[19] J. Seidel, S. Grafström, and L. Eng, "Stimulated emission of surface plasmons at the interface between a silver film and an optically pumped dye solution," *Phys. Rev. Lett.*, vol. 94, no. 17, pp. 117401-1–117401-4, 2005.
[20] A. Tredicucci, C. Gmachl, F. Capasso, A. L. Hutchinson, D. L. Sivco, and A. Y. Cho, "Single-mode surface-plasmon laser," *Appl. Phys. Lett.*, vol. 76, no. 16, pp. 2164–2166, 2000.
[21] J. J. Burke, G. I. Stegeman, and T. Tamir, "Surface-polariton-like waves guided by thin, lossy metal films," *Phys. Rev. B*, vol. 33, no. 8, pp. 5186–5201, 1986.
[22] S. J. Al-Bader and M. Imtaar, "Azimuthally uniform surface-plasma modes in thin metallic cylindrical shells," *IEEE J. Quantum Electron.*, vol. 28, no. 2, pp. 525–533, Feb. 1992.
[23] K. A. Shore, "Modulation bandwidth of metal-clad semiconductor nanolasers with cavity-enhanced spontaneous emission," *Electron. Lett.*, vol. 46, no. 25, pp. 1688–1689, Dec. 2010.
[24] V. E. Babicheva, I. V. Kulkova, R. Malureanu, K. Yvind, and A. V. Lavrinenko, "Plasmonic modulator based on gain-assisted metal-semiconductor-metal waveguide," *Semicond. Sci. Technol.*, vol. 7, pp. 858–860, May 2012.
[25] P. B. Johnson and R. W. Christy, "Optical constants of the noble metals," *Phys. Rev. B*, vol. 6, no. 12, pp. 4370–4379, Dec. 1972.

[26] P. Bhattacharya, *Semiconductor Optoelectronic Devices*, 2nd ed. Englewood Cliffs, NJ, USA: Prentice-Hall, 1997.
[27] D. Cui, S. M. Hubbard, D. Pavlidis, A. Eisenbach, and C. Chelli, "Impact of doping and MOCVD conditions on minority carrier lifetime of zinc- and carbon-doped InGaAs and its applications to zinc- and carbon-doped InP/InGaAs heterostructure bipolar transistor," *Semicond. Sci. Technol.*, vol. 17, pp. 503–509, May 2002.
[28] P. Ambree, B. Gruska, and K. Wandel, "Dependence of the electron diffusion length in p-InGaAs layers on the acceptor diffusion process," *Semicond. Sci. Technol.*, vol. 7, pp. 858–860, Apr. 1992.
[29] R. B. Lee, K. J. Vahala, C. Zah, and R. Bhat, "Direct determination of the ambipolar diffusion length in strained $In_xGa_{1-x}As/InP$ quantum wells by cathodoluminescence," *Appl. Phys. Lett.*, vol. 62, no. 19, pp. 2411–2412, May 1993.
[30] L. A. Coldren and S. W. Corzine, *Diode Lasers and Photonic Integrated Circuits*, 1st ed. New York, NY, USA: Wiley, 1995.
[31] A. V. Maslov and C. Z. Ning, "Reflection of guided modes in semiconductor nanowire lasers," *Appl. Phys. Lett.*, vol. 83, no. 6, pp. 1237-1–1237-3, 2003.
[32] K. Ding and C. Z. Ning, "Metallic subwavelength-cavity semiconductor nanolasers," *Light, Sci. Appl.*, vol. 1, no. 7, pp. 1–20, Jul. 2012.

Zubaida Abdul Sattar (S'12) received the bachelor's degree in electronic engineering from the Sir Syed University of Engineering and Technology, Karachi, Pakistan, in 2009, and she is currently pursuing the Ph.D. degree in electronic engineering with Bangor University, U.K.

Her research interest includes theoretical investigation of optical properties towards the design of semiconductor nano-lasers and she has delivered many talks in international conferences.

Ms. Sattar is a student member of EOS and IOP, and a Vice President of the SPIE Student Chapter at Bangor University, U.K., from 2013 to 2014. She is the Chair of the IEEE Student Branch at Bangor University.

Zengbo Wang received the B.Sc. and M.Sc. degrees in physics from Xiamen University, China, in 1997 and 2001, respectively, and the Ph.D. degree in electrical and computer engineering from the National University of Singapore (NUS), Singapore, in 2005.

He was a Senior Research Fellow and the recipient of the Most Outstanding Research and Development Staff Award 2005 at Data Storage Institute, Singapore from 2005 to 2006, a Post-Doctoral Research Fellow at The University of Manchester from 2006 to 2008 and The University of Southampton from 2008 to 2009. In 2009, he was a Lecturer of laser micro nano engineering with The University of Manchester. He was with the School of Electronic Engineering, Bangor University, in 2012, as a Senior Lecturer of imaging and nanophotonics. His expertise lies in the fields of optical nanoscopy and imaging, nano-fabrication, nano-plasmonics/electronics, laser micro nano processing, laser cleaning and the applications. He has author or co-authored more than 90 publications (WOS H-index: 13), including high-impact papers in nature and physics review journals, and has delivered more than 20 invited talks in major international conferences.

Dr. Wang is the main inventor of the world's first 50-nm resolution white-light nanoscope that could be potentially used for virus imaging in real time. The work, published in Nature Communications, has attracted huge public interests and media coverage including BBC, New York Times, and Daily Mail. It was awarded a first prize in a Royal Academy of Engineering Poster Competition Event in nano-engineering, invited as a feature article in Laser Focus World, and honored by the RCUK as one of 50 big ideas for the future in year 2011.

K. Alan Shore (SM'95) received the Graduate degree in mathematics from the University of Oxford, Oxford, U.K., and the Ph.D. degree from the University College, Cardiff, Wales, U.K.

He was a Lecturer at the University of Liverpool from 1979 to 1983 and then at the University of Bath where he became a Senior Lecturer in 1986, Reader in 1990, and Professor in 1995. He was a Visiting Researcher with the Center for High Technology Materials, University of New Mexico, Albuquerque, NM, USA, in 1987. In 1989, he was a Visiting Researcher at Leiden University, The Netherlands. In 1990 and 1991, he was with the Teledanmark Research Laboratory and the MIDIT Center of the Technical University of Denmark. He was a Guest Researcher at the Electrotechnical Laboratory, Tsukuba, Japan, in 1991. In 1992, he was a Visiting Professor at the Department of Physics, University de les Illes Balears, Palma-Mallorca, Spain. He was a Visiting Lecturer with Instituto de Fisica de Cantabria, Santander, Spain, in 1996 and 1998, and was a Visiting Researcher at Macquarie University, Sydney, Australia, in 1996, 1998, 2000, 2002, 2005, and 2008. In 2001, he was a Visiting Researcher at the ATR Adaptive Communications Laboratories, Kyoto, Japan. In 1995, he joined Bangor University where he was the Head of the School of Informatics and the College of Physical and Applied Sciences. In 2001 and 2008, he was the Director of the Industrial and Commercial Optoelectronics, a Welsh Development Agency Centre of Excellence. He was the Chair of the Welsh Optoelectronics Forum from 2006 to 2008 and has been a Chair of the Photonics Academy for Wales since 2005. From 2008 to 2011, he was the Chair of the Quantum Electronics Commission of the International Union of Pure and Applied Physics. His research work has been principally in the area of semiconductor optoelectronic device design and experimental characterization with particular emphasis on nonlinearities in laser diodes and semiconductor optical waveguides. He has authored or co-authored more than 900 contributions to archival journals, books, and technical conferences. He has co-edited the research monograph *Unlocking Dynamical Diversity*. His current research interests include the dynamics of vertical-cavity semiconductor lasers, applications of nonlinear dynamics in semiconductor lasers, and the design of nano-spin semiconductor lasers.

Prof. Shore co-founded and has been the Organizer and Program Committee Chair for the International Conference on Semiconductor and Integrated Optoelectronics, Cardiff, Wales, U.K., since 1987. He was a Program Member for several OSA conferences and was a co-organizer of a Rank Prize Symposium on Nonlinear Dynamics in Lasers at Lake District, U.K., in 2002. He was a Chair of the Education and Training in Optics and Photonics conference at Technium OpTIC, Wales, in 2009. He received the Royal Society Travel Grant to visit universities and laboratories in Japan in 1988. In 2010, he held a Japan Society for the Promotion of Science Invitation Fellowship in the Ultrafast Photonics Group, Graduate School of Materials Science, Nara Institute of Science and Technology, Nara, Japan. He is a fellow of the Optical Society of America, the Institute of Physics, and the Learned Society of Wales. He has been serves as a Council Member since 2012.